

IONOSPHERIC NETWORK ADVISORY GROUP (INAG)*

INAG BULLETIN NO. 42**

An Atlas of Ionograms

A reference collection of ionograms from high
latitude observatories

Compiled by A S Besprozvannaya and T I Shchuka

* Under the auspices of Commission G, working
group G1 of the International Union of
Radio Science (URSI).

** Prepared by A S Rodger, British Antarctic
Survey, Madingley Road, Cambridge, CB3 0ET,
UK. Issued on behalf of INAG by the World
Data Center - A for Solar Terrestrial Physics,
National Oceanic and Atmospheric Administration,
Boulder, Colorado 80303, USA. This bulletin
is distributed to ionospheric stations by
the same channels (but in the reverse direction)
as their data ultimately flow to WDC-A.
Others wishing to be on the distribution
list of the INAG Bulletin should notify WDC-A.

1. INTRODUCTION TO THE ATLAS

by A S Rodger, S M Broom and R W Smith

The Atlas of Ionograms compiled by A S Besprozvannaya and T I Shchuka of the Ionogram Reduction Group at the Geophysical Department of the Arctic and Antarctic Research Institute, Leningrad, USSR forms the entire INAG Bulletin. This Atlas should form a very valuable reference manual for those involved in ionogram interpretation and for scientists who used ionogram data in their research.

A few minor modifications to the original script have been made to make the scaling procedures more in accord with those recommended in the Handbooks of Ionogram Interpretation and Reduction and that used in the INAG Bulletins. A fuller discussion of the differences between the practices in the USSR and the standard INAG recommendations has been given in INAG 35 pp 3-6. Since most groups have not taken advantage of the simplifications made at Washington (eg, the combining of Es-r and Es-k) the examples have been modified to be consistent with the original practise.

There is an additional local rule regarding the scaling of range spread-F adopted in the USSR. Range spread-F is divided into two groups, unresolved range spread-F, Q, and resolved range spread-F, Q1, with trough-ridge traces being incorporated into the latter group. The differences in these patterns results from the size of the reflecting structures. Structures with small horizontal size give unresolved range spread-F, medium scale features give resolved range spread-F and large structures give trough-ridge sequences. The two main features which comprise a trough-ridge structure are very different whereas those which form medium and small scale structure are much more similar in shape (see UAG-23A, Fig. 2.15 and 2.22). However, in the text we have kept the USSR interpretation but request the views of other groups on whether range spread-F should be comprised of one, two or three types (i.e., all range spread-F one group; Q and Q1 as given in this Atlas or resolved range spread-F, unresolved range spread-F and trough-ridge sequences).

We have also added a few additional comments to clarify why specific scalings have been adopted, or to provide further explanation of the ionogram sequences.

Ionograms from several observatories are used in this Atlas. The table below lists these stations together with their geophysical location.

| | Geographic | | Geomagnetic | | L-shell |
|--------------|------------|-----------|-------------|-----------|---------|
| | lat | long east | lat | long east | |
| DIXON | 74 | 80 | 63 | 162 | 6.9 |
| HEISS | 81 | 58 | 71 | 156 | 14.1 |
| MIRNY | -66 | 93 | -77 | 148 | 20.8 |
| MOSCOW | 55 | 37 | 51 | 121 | 2.5 |
| NARSSARSUAK | 61 | 315 | 71 | 37 | 7.1 |
| NORTH POLE-8 | 80 | 165 | 70 | 205 | 13 |
| TIKSI | 72 | 129 | 60 | 192 | 5.6 |
| VOSTOK | -78 | 107 | -89 | 94 | 72 |

One further, more conventional, INAG Bulletin should be produced before the URSI General Assembly in Florence. However, there is still a great shortage of station notes, ionogram sequences, articles of historical or scientific interest. Please send

your contributions to the Secretary as soon as you can.

2. AN ATLAS OF IONOGRAMS

by A S Besprozvannaya and T I Shchuka

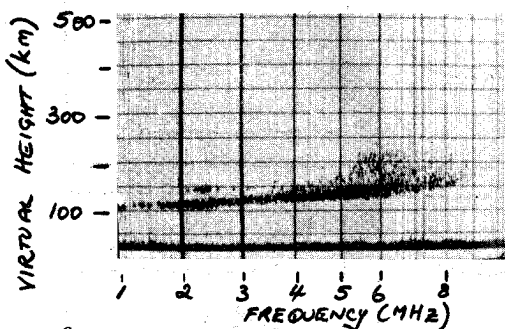
This Atlas has been prepared as a reference-book to be used for scaling and interpretation of high-latitude ionograms which reflect the specific polar ionosphere conditions. The Atlas has been compiled with the two objectives in mind: to help in the correct identification of the observed events and to facilitate making their scaling identical using the existing URSI rules and procedures.

The Atlas contains examples of ionograms corresponding to different station positions with respect to the main ionospheric trough and particle precipitation responsible for discrete and diffuse aurorae. The complexity in determining the parameters of high latitude sporadic ionization in the E region and their interpretation and reduction of spread traces in F region are dealt in greater detail.

The Atlas has been prepared in the Geophysical Department of the Arctic and Antarctic Research Institute, Leningrad, USSR, in accordance with the INAG recommendation to prepare reference material for training the operators of high-latitude ionospheric stations. The ionogram reduction has been carried out in accordance with the URSI Handbook with consideration of modifications and additions adopted at the Soviet National Workshops devoted to the ionogram interpretation and reduction.

The Atlas is primarily addressed to those concerned with the reduction of vertical sounding ionograms and to scientists who make use of ionospheric data in their research.

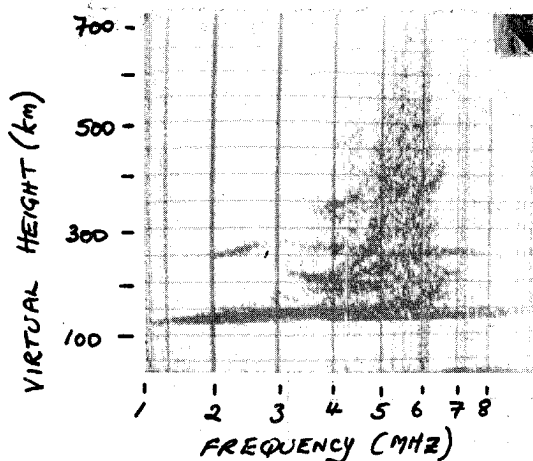
Figure 1 - An example of auroral Es (Es-a)



Dixon 1970 10 July 0300LT (105°E)

| foE | foEs | fbEs | h'Es | Es type |
|-----|-------|-------|------|---------|
| A | 076JA | 076AA | 105 | al |

Figure 2

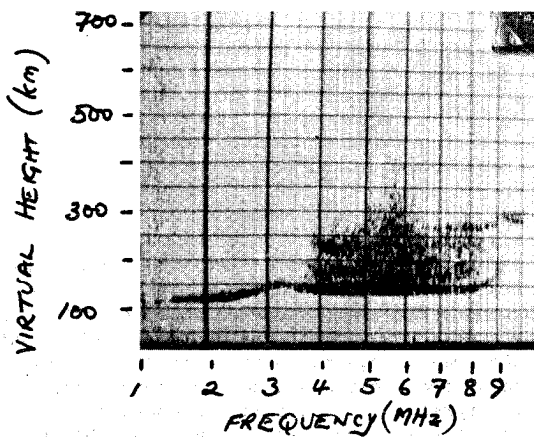


Dixon 1970 2 January 2015LT (105°E)

| foEs | fbEs | h'Es | Es type |
|-------|-------|------|---------|
| 080JA | 030-K | 125 | a2k2 |

Comment: This night-time ionogram shows a weak F-region trace with h'F at 200 km and foF2 at about 5.2 MHz. This is a relatively rare example of Es-a traces superposed on Es-k. Note the retardation on the second order Es-k trace and the low-frequency end of the F-trace.

Figure 3

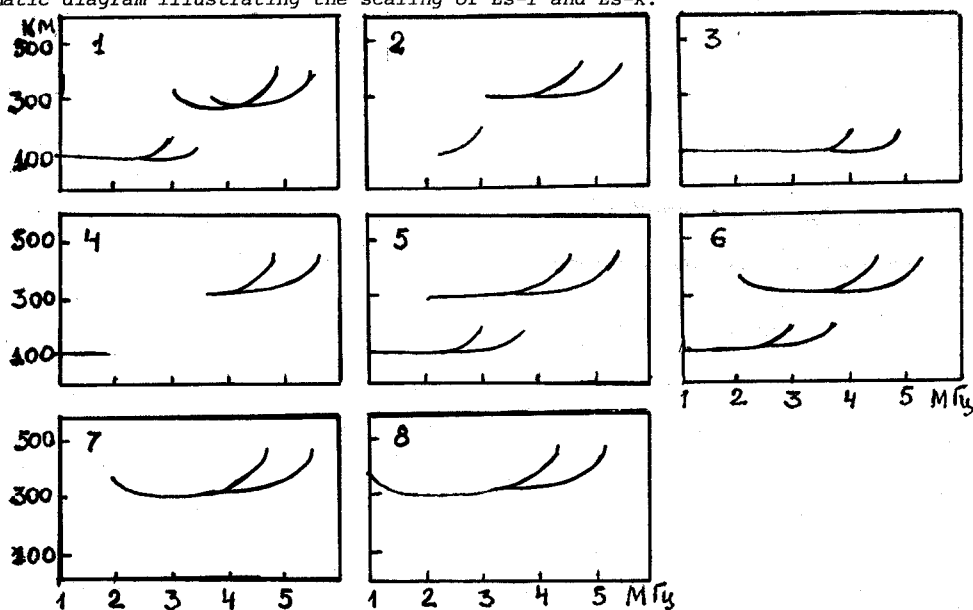


Dixon 1970 29 July 1715LT (105°E)

| foE | foEs | fbEs | h'Es | Es type |
|-------|-------|-------|------|---------|
| 350UA | 082JA | 082AA | 130 | al |

Comment: There is a small turn up at the high frequency end of the Es-a trace. In principle, this could be scaled as Es-r but Es-a was chosen as it provides a more accurate description of the entire Es trace, and indicates the considerable spreading present.

Figure 4 Schematic diagram illustrating the scaling of Es-r and Es-k.



| | Tabulation | | | f plot symbol | |
|---|------------|-------|---------|---------------|---------|
| | foEs | fbEs | type Es | fbEs | type Es |
| 1 | O30-K | O30-K | kl | ○ | ○ |
| 2 | O30-Y | O30-Y | rl | ◆ | ● |
| 3 | O40-K | O40AK | kl | ◆ | ○ |
| 4 | Y | Y | kl | Y | ● |
| 5 | O30 | O20 | rl | ◆ | ○ |
| 6 | O30 | O20-K | rl | ○ | ○ |
| 7 | O2OEB | O2OEK | - | - | - |
| 8 | O1OEE | O1OEK | - | - | - |

Comment: Each Es trace at 100 km is assumed to be a reflection from an Es layer.

Example 2: This pattern of traces is quite unusual. Although there is a turn up at the high-frequency end of the Es-trace, there is no corresponding turn down at the low frequency end of the F-trace which begins at foEs. This indicates that a significant tilt must be present in either the Es or F layers or indeed both. The descriptive letter Y on foEs and fbEs has been used to show the presence of this tilt. Under these circumstances, distinction between Es-k and Es-r is not possible (this illustrates one reason why combining k and r types was allowed at Washington). The choice of Es type should be made using the sequence of ionograms or the second order traces if there are any present.

Example 3: This is another occasion when it is difficult to decide whether to scale as Es-r or Es-k. The presence of an x-mode trace often

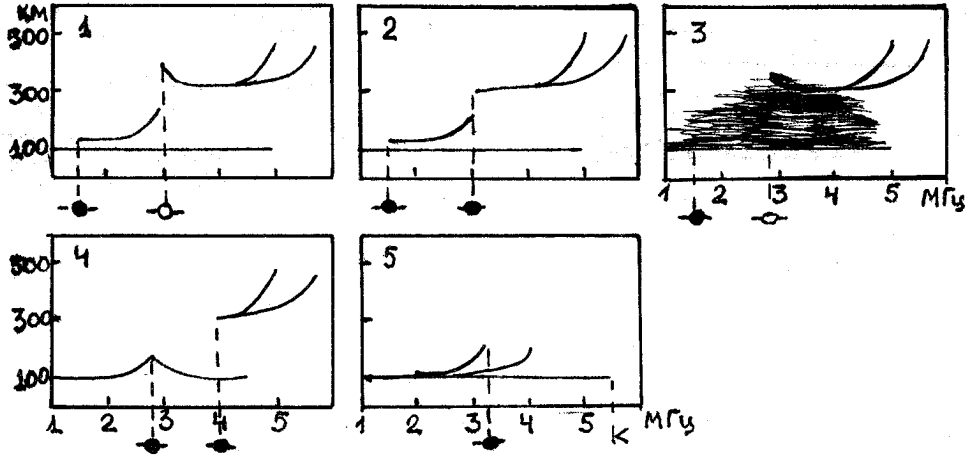
indicates Es-k is more likely. Second order traces can also be helpful. If this is seen up to a frequency close to foEs, then Es-k is scaled. However, if the second order extends over the lower frequency part of the first order trace only, then Es-r would be more appropriate. This interpretation is similar in approach to that for thin Es-layers which completely blanket (see figures 3.1 and 3.2 of UAG-23A).

Example 4: There is really insufficient evidence available to determine which type of Es is present without using the sequence of ionograms, but the example is intended to illustrate lacuna with the retardation near foEs cut off by the lacuna.

Examples 6-8: The use of the descriptive letter K with fbEs is a very effective way of inducting the effects of an Es-k layer which is not actually observed on the ionograms.

Figure 4a Schematic diagram illustrating the scaling of Es parameters when two Es layers are present.

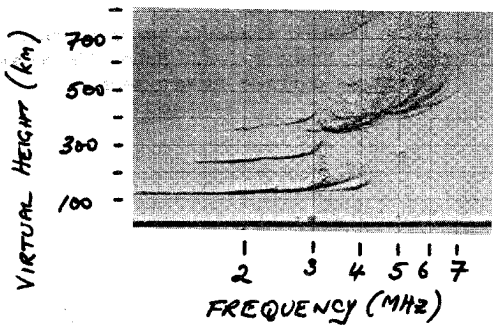
In each of these examples, two Es layers are present and one of them has group retardation at the high-frequency end. The layer with the highest value of foEs should be scaled and all Es parameters must be scaled from the same layer. Again the descriptive letters K on fbEs has been used to indicate the presence of an Es-k layer. Note, if the low Es is a weak trace, it should be ignored in accordance with the rules (see Handbook Chapter 2).



| | foEs | fbEs | type Es |
|---|-------|-------|---------|
| 1 | 042JA | 015-K | 11k1 |
| 2 | 042JA | 030-- | 11r1 |
| 3 | 042JA | 015-K | a1k1 |
| 4 | 045-- | 040-- | c1k1 |
| 5 | 047JA | 020-K | 11k1 |

Figures 5 - 8 These ionograms show similarities to the line diagrams provided in Figure 4 examples 1, 2 and 5, and to Figure 4a example 4 respectively.

Figure 5



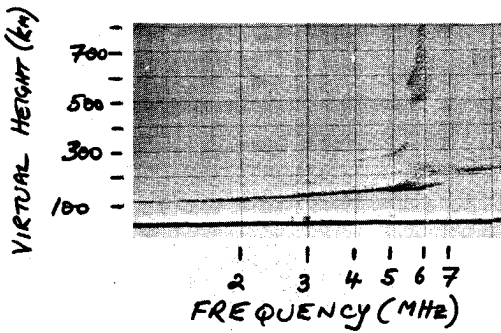
Tiksi 1958 7 September 2045LT (135°E)

foEs fbEs h'Es Es type
030-K 030-K 115 k3s1

foF2 h'F fxI type F
048DF 350Q 070 FQ

Comment: There is an Es-s trace present extending above 3.0 MHz. This should not be used to determine Es parameters but only appears in the Es-types column

Figure 6



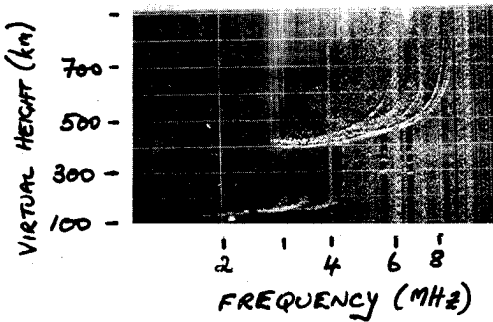
Tiksi 1958 3 September 2145LT (135°E)

| foEs | foEs | h'Es | Es type |
|------|------|------|---------|
| 056 | 053 | 100 | r2 |

| foF2 | h'F | fxI | type F |
|-------|-----|-------|--------|
| 059UF | A | 0680B | F |

Comment: There is a weak Es-a trace above 6.0MHz and with a virtual height in excess of 200 km. It has been omitted from the scaling, as to include it would lead to a misrepresentation of the overhead ionosphere.

Figure 7



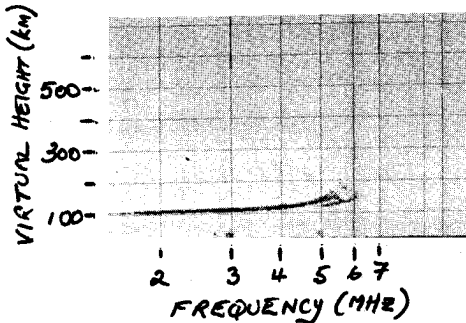
Narssarsuak 1958 3 January 1930LT (45°W)

| foEs | fbEs | h'Es | Es type |
|------|------|------|---------|
| 034 | 027 | 110 | r1 |

| foF2 | h'F | fxI | type F |
|-------|-----|-----|--------|
| 060UF | 400 | 085 | F |

Comment: The scaling of foF2 in this case is difficult. In the original manuscript foF2 was given as 060UF. However, the strongest F-region critical is at 8.0 MHz. The sequence of ionograms would probably resolve the problem.

Figure 8

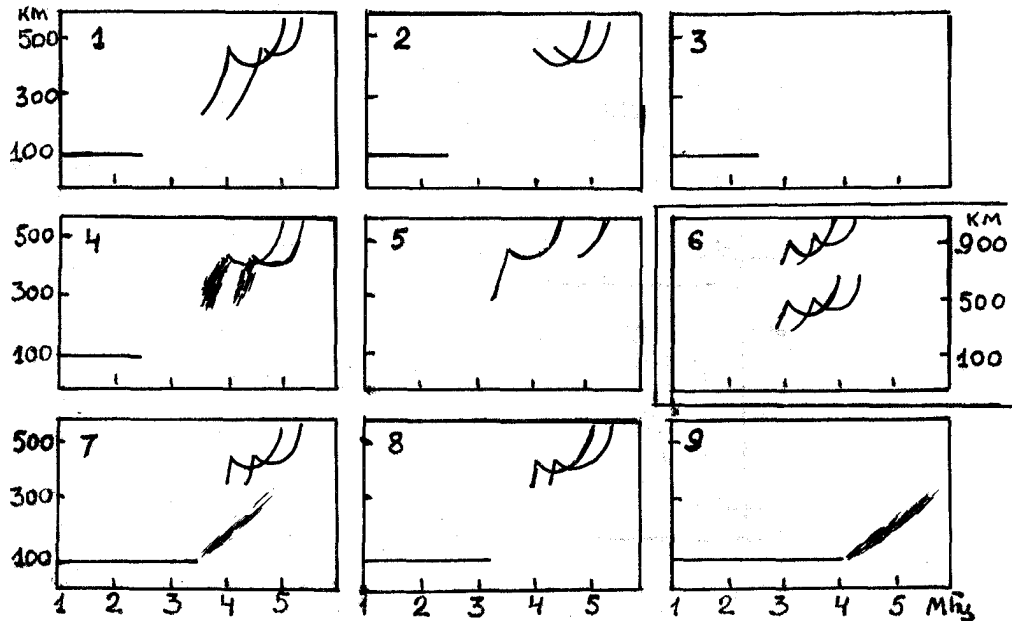


Tiksi 1958 30 June 0400LT (135°E)

| foEs | fbEs | h'Es | Es type |
|-------|-------|------|---------|
| 054-K | 054-K | 100 | kl |

Comment: The weak Es-c trace is ignored under the weak trace rules. Note, the x-mode of the Es-c trace is not seen.

Figure 9 Ionogram scaling for examples of lacuna



| | fmin | foE | foEs | fbEs | foF2 | foF1 | h'F2 | h'F | type Es |
|---|-------|-----|-------|-------|------|-------|------|-------|---------|
| 1 | O1OEE | Y | O3OEG | O3OEG | O50 | 400 | 400 | 250EY | - |
| 2 | O1OEE | Y | O3OEG | O3OEG | O50 | 400EY | 400 | Y | - |
| 3 | O1OEE | Y | O3OEG | O3OEG | Y | Y | Y | Y | - |
| 4 | O1OEE | Y | O3OEG | O3OEG | O50 | 400UF | 400 | Y | - |
| 5 | O32 | B | O32EB | O32EB | O45 | 350 | 450 | B | - |
| 6 | O28-Y | Y | O32EY | O32EY | O40 | 300 | 450 | Y | - |
| 7 | O1OEE | A | O35 | Y | O50 | 400 | 400 | Y | 11s1 |
| 8 | O1OEE | A | Y | Y | O50 | 400 | 400 | Y | 11 |
| 9 | O1OEE | A | O42-Y | O42EY | Y | Y | Y | A | 11s1 |

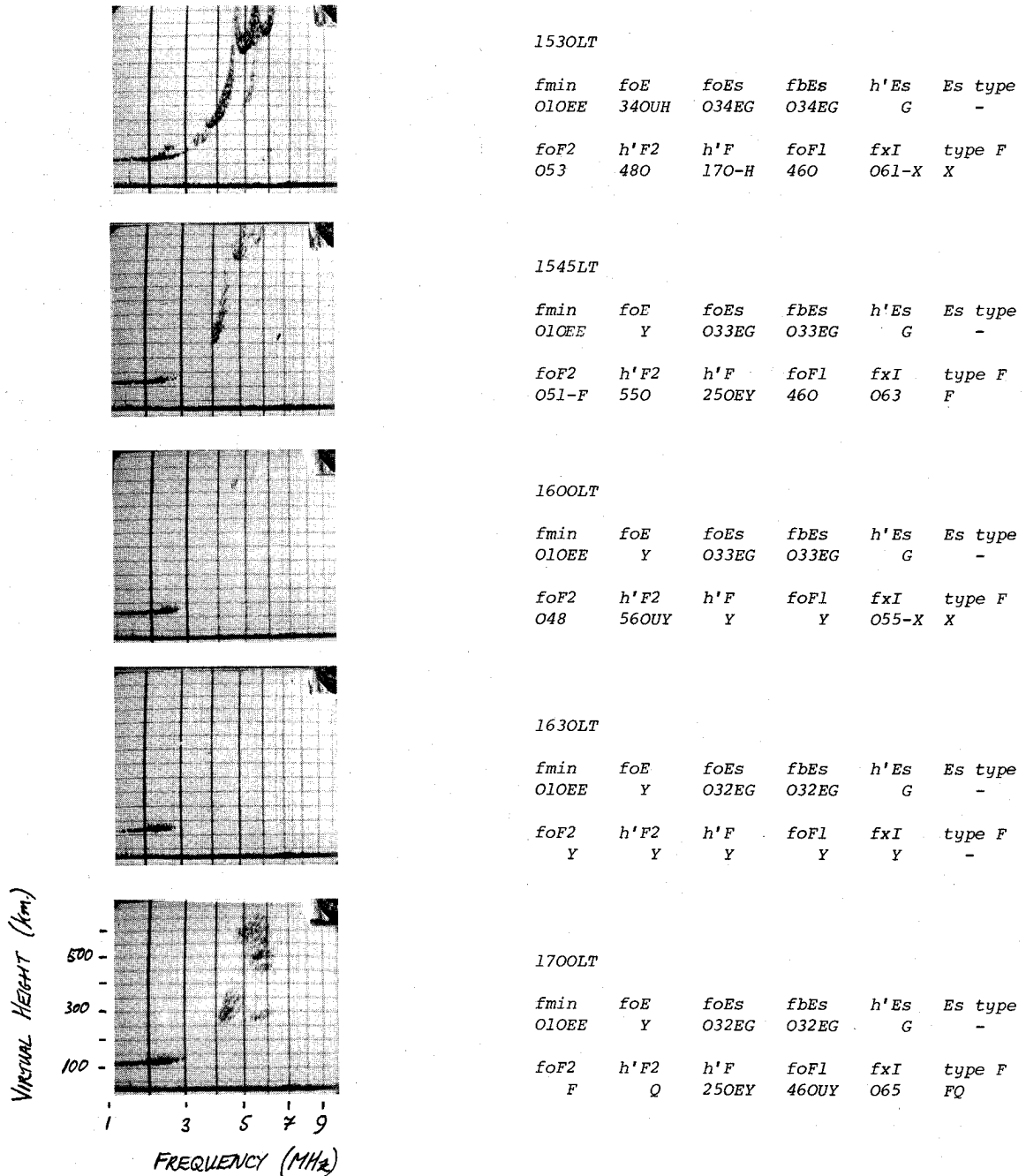
Comments

Examples 1-4. It is assumed that the traces at 100 km are normal E region reflections and foE is 3.0 MHz.

Examples 5-6. These examples are included to illustrate the differences between the absence of E and lower F region traces caused by high absorption (Example 5) and lacuna (Example 6). The key differences are that the x-mode F-region trace shows considerable absorption also with $f_{min} f_x \gg f_{min} f_o + f_B/2$ for example 5. In contrast, example 6 shows $f_{min} f_x = f_{min} f_o + f_B/2$. Also second order F region traces are observed in the latter case, hence lacuna is the most probable explanation for the missing traces.

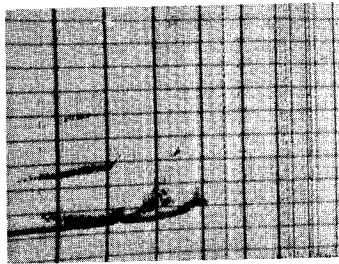
Examples 7-9. It is assumed that the traces at 100 km are from Es layers for these cases. Analogous patterns can arise from a normal E trace e.g., UAG-23A Figure 2.19.

Figure 10 A sequence of ionograms from Dixon on 9 July 1970 showing the evolution of lacuna.



Comment: The ionograms of 1545, 1600 and 1780 show partial lacuna, while the ionogram at 1630 shows total lacuna. At 1700, the descriptive letter Y has been used in preference to F with foF1 to illustrate that lacuna is the more important reason for the difficulty in scaling.

Figure 11 Examples of lacuna from Dixon on the 11 December 1970

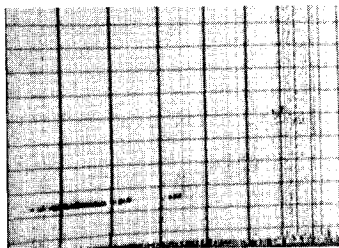


1530LT

| | | | |
|-------|-------|-------|---------|
| foEs | fbEs | h'Es | Es type |
| 040-K | 040AA | 100-Z | kl |

| | | | |
|------|-----|-----|--------|
| foF2 | h'F | fxI | type F |
| A | A | A | - |

Comment: There is a slight indication that an Es-c layer may also be present. This has been ignored under the scaling on the weak and intermittent trace rule (UAG 23-A, p 29). A z-o-x triplet is present with very low absorption of the Z-trace. As Es type scaling is taken from the o-mode trace kl is used.

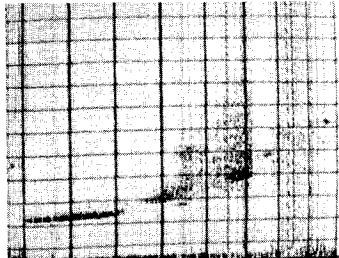


1545LT

| | | | |
|------|------|------|---------|
| foEs | fbEs | h'Es | Es type |
| Y | Y | 110 | kl |

| | | | |
|------|-----|-----|--------|
| foF2 | h'F | fxI | type F |
| A | A | A | - |

Comment: There is insufficient evidence on this ionogram alone to be sure of the Es type. Es-k is used to maintain the continuity.

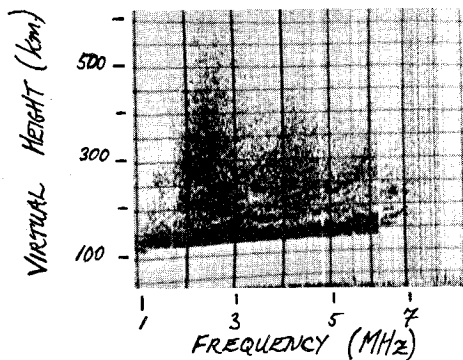


1600LT

| | | | |
|------|-------|------|---------|
| foEs | fbEs | h'Es | Es type |
| 060 | 034EK | 145 | alkl |

| | | | |
|------|-----|-----|--------|
| foF2 | h'F | fxI | type F |
| A | A | A | - |

Comment: Es-a is preferred as it indicates that very diffuse and spread traces are present.



1630LT

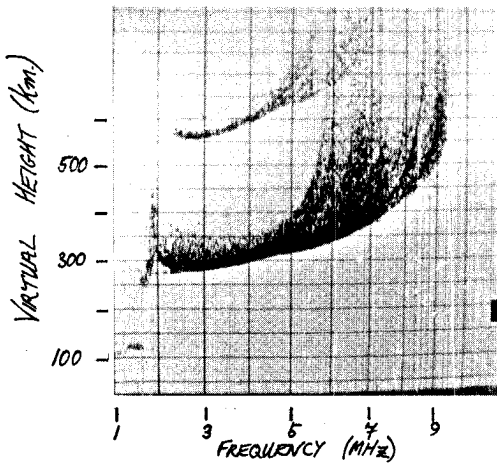
| | | | |
|-------|-------|------|---------|
| foEs | fbEs | h'Es | Es type |
| 062JA | 062AA | 120 | al |

| | | | |
|------|-----|-----|--------|
| foF2 | h'F | fxI | type F |
| A | A | A | - |

Comment: In each of these examples foF2 is expected to be below the top frequency of the blanketing Es layers. This sequence is typical of that observed in the auroral zone in the daytime during winter months under geomagnetically disturbed conditions.

Figures 12-14 These ionograms illustrate frequency, range and mixed spread-F (UAG 23A p58)

Figure 12



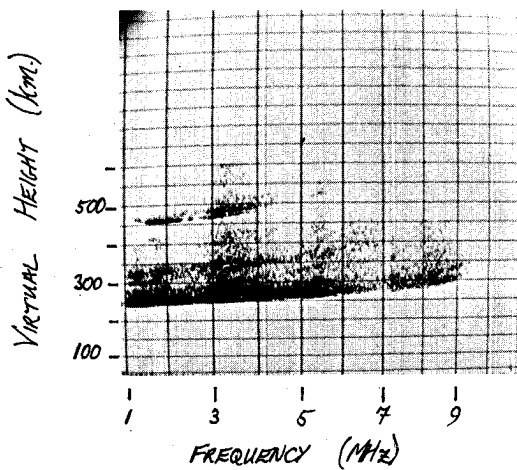
Mirny 1970 21 June 1215 (90°E)

| foE | foEs | fbEs | h'Es | Es type |
|-----|-------|-------|------|---------|
| 190 | 019EG | 019EG | G | - |

| foF2 | h'F | fxI | type F |
|-------|-----|-----|--------|
| 058UF | 275 | 092 | F |

Comment: At high geographic latitudes, normal E is often seen at heights near 200 km when the sun is below or close to the horizon at the earth's surface. Day to day sequence allows correct identification of foE.

Example 13

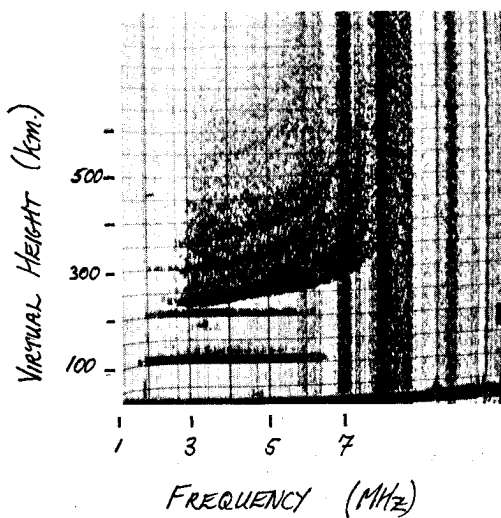


Vostok 1970 23 June 1400 (105°E)

| foF2 | h'F | fxI | type F |
|------|-------|-----|--------|
| Q | 250-Q | 093 | Q |

Comment: An example of range spread-F. As the USSR uses Q1 for resolved range spread-F, QQ1 could be an acceptable spread-F scaling here to indicate that both unresolved and resolved range spread-F are present.

Example 14



Mirny 1970 28 January 2345 (90°E)

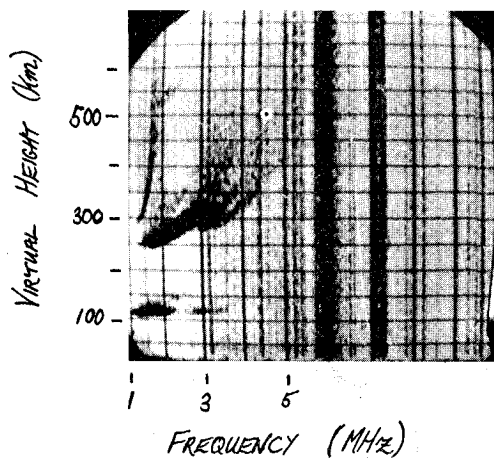
| foEs | fbEs | h'Es | Es type |
|-------|------|------|---------|
| 045JA | 017 | 100 | f3 |

| foF2 | h'F | fxI | type F |
|------|-------|-------|--------|
| F | 225-Q | 070DS | FQ |

Comment: Both range and frequency spread-F are present. This combination could be classified as spread-F type L (UAG-23A p58).

Figures 15-17. Further illustrations of spread-F typing including the polar spur (P).

Figure 15

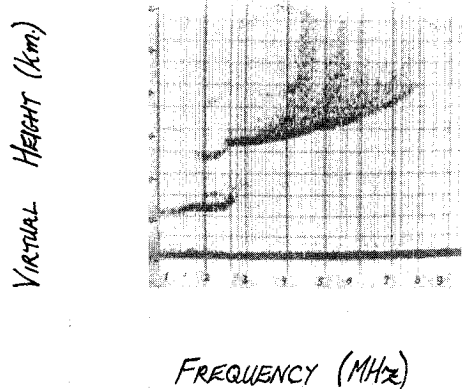


Norilsk 1967 14 December 0400 (90°E)

| | | | |
|------|------|------|---------|
| foEs | fbEs | h'Es | Es type |
| 022 | 013 | 105 | f1 |
| foF2 | h'F | fxI | type F |
| 018 | A | 060 | PX |

Comment: This is part of trough-ridge sequence of ionograms. The sequence would help considerably in determining which of the two F layer is chosen as overhead. In this case, the lower frequency F-layer is scaled as the overhead layer.

Figure 16

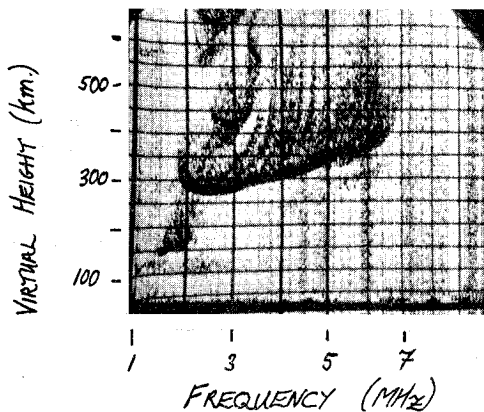


Dixon 1969 13 February 1710 (105°E)

| | | | |
|-------|------|------|---------|
| foEs | fbEs | h'Es | Es type |
| 027 | 025 | 110 | r2 |
| foF2 | h'F | fxI | type F |
| 044UF | 320 | 080 | PF |

Comment: This example shows similarities to examples 2 and 5 on Figure 4.

Figure 17

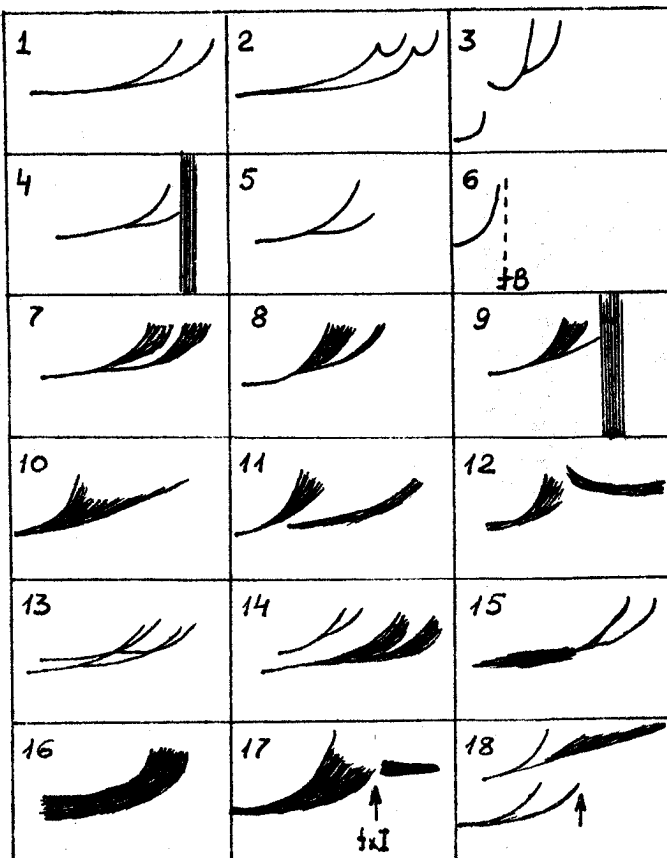


Dixon 1978 20 February 1705 (105°E)

| | | | |
|-------|-------|-------|--------|
| foE | foEs | fbEs | h'Es |
| 180UF | 018EG | 018EG | G |
| foF2 | h'F | fxI | type F |
| 039UF | 270 | 070 | Q1F |

Comment: Q1 is used to indicate resolved range spread-F. See introduction for further discussion of the spread-F typing under these circumstances.

Figure 18 The scaling of fxI



| | foF2 | fxI | h'F | type F | | foF2 | fxI | h'F | type F |
|---|-------|-------|-------|--------|----|-------|-------|-------|--------|
| 1 | O44 | O52-X | 250 | X | 10 | O35-F | O70 | 250 | PF |
| 2 | O44-H | O52-X | 250 | X | 11 | O35-F | O70 | 250 | PF |
| 3 | O38EG | O46-X | 250 | X | 12 | O35-F | O70 | 250 | PF |
| 4 | O44 | O52OS | 250 | X | 13 | O44 | O53-X | 250 | XQI |
| 5 | O44 | O52OR | 250 | X | 14 | O44-F | O60 | 250 | FQI |
| 6 | O1O | O17OB | 25OEE | X | 15 | O44 | O52-X | 250-Q | XQ |
| 7 | O44-F | O57 | 250 | F | 16 | F | O60 | 250-Q | FQ |
| 8 | O44-F | O56OR | 250 | F | 17 | O44UF | O60 | 250 | F |
| 9 | O44-F | O56OS | 250 | F | 18 | O44 | O52-X | 250 | X |

Comment: It is stressed that the scaling of spread-F is indicated here in a separate column. Thus there are many differences from the scheme proposed in INAG Bulletin 33, pp 32-33 where the presence of spread-F was given in the standard parameter tables. $fb/2 = 0.8$ MHz for these examples.

Example 3. Only an F1 layer present, F2 in G condition.

Example 11 and 14. In example 11, the oblique trace has a higher critical frequency than the overhead layer and is classified as a polar spur (P). In example 14, the oblique trace is at a frequency lower than foF2; thus the spread-F type is scaled as QI indicating resolved range spread-F.

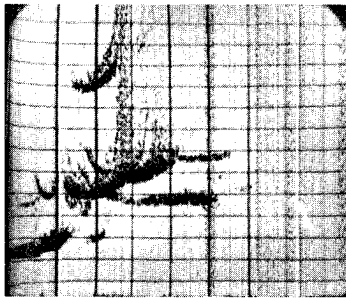
Example 17. The second trace at a higher frequency due to an oblique Es-a trace not a polar spur, which is why fxI is not scaled from the top frequency. The sequence of ionograms is normally of great benefit in resolving oblique Es-a from a polar spur trace (see Figure 19 for example).

Example 18. A backscatter trace from the earth's surface occurring only on second order traces. It is neglected for the purposes of scaling fxI .

Figure 19 An oblique Es-a trace causing difficulty in scaling fxI.

The example below from Heiss on 7 March 1977 illustrates the difficulty which can be experienced in determining fxI when oblique Es-a traces are present. The sequence of ionograms is very important under these circumstances. This sequence also shows the movement of the auroral oval with respect to the observatory.

The Handbook does not provide specific criteria for deciding when foEs should be scaled from Es-a layers. The height of the layer varies very rapidly with time and a criterion which can be adopted is to scale it when h'Es is less than h'F. In this sequence the criterion adopted for scaling Es-a is to measure it when h'Es is clearly less than 200 km. The main difficulty, well illustrated by the example, is that foEs nearly always increases with the obliquity of the Es-a, so there is an apparent conflict between picking foEs from the layer with the greatest value and the basic rule of scaling to measure the ionosphere nearest overhead. In this situation, the chairman would use the lowest Es-a trace for analysis.



1230LT

| foE | foEs | fbEs | h'Es | Es type |
|-------|-------|-------|--------|---------|
| 210 | O21EG | O21EG | G | - |
| foF2 | h'F | fxI | type F | |
| O38-F | 245-H | O51 | F | |

Comment: The second order F-trace has been used to determine foF2. In case of these examples on p13, there is a z-mode normal E region trace present. Its presence could be indicated with the h'E value.



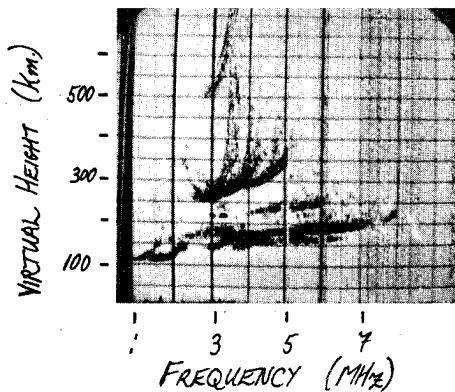
1245LT

| foE | foEs | fbEs | h'Es | Es type |
|-------|-------|-------|--------|---------|
| 205 | O20EG | O20EG | G | - |
| foF2 | h'F | fxI | type F | |
| O37-F | 240 | O53 | F | |



1255LT

| foE | foEs | fbEs | h'Es | Es type |
|-------|-------|-------|--------|---------|
| 205 | O82JA | O20EG | 160 | a1 |
| foF2 | h'F | fxI | type F | |
| O36-F | 240 | O60 | F | |

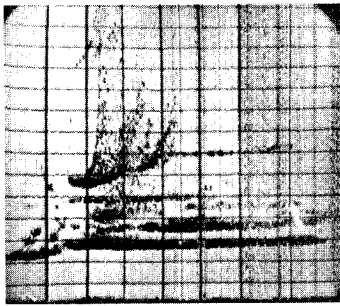


1300LT

| foE | foEs | fbEs | h'Es | Es type |
|-------|-------|------|--------|---------|
| 205 | O72JA | O25 | 150 | a1 |
| foF2 | h'F | fxI | type F | |
| O34-F | 250 | O52 | F | |

Comment: Despite the turn-up at the high-frequency end of the Es-trace, Es-a has been scaled to indicate the structure present.

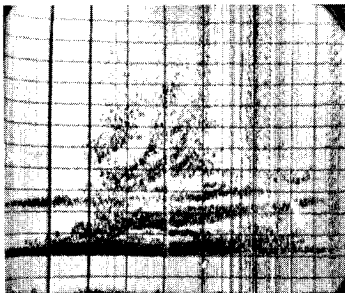
Figure 19 continued. Heiss 7 March 1977



1315LT

| foE | foEs | fbEs | h'Es | Es type |
|-----|-------|------|------|---------|
| 200 | 084JA | 025 | 130 | al |

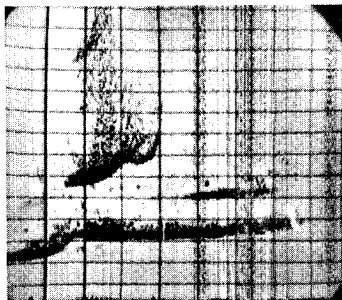
| foF2 | h'F | fxI | type F |
|-------|-----|-----|--------|
| 032UF | 270 | 055 | F |



1345LT

| foE | foEs | fbEs | h'Es | Es type |
|-----|-------|------|------|---------|
| A | 092JA | 030 | 100 | al |

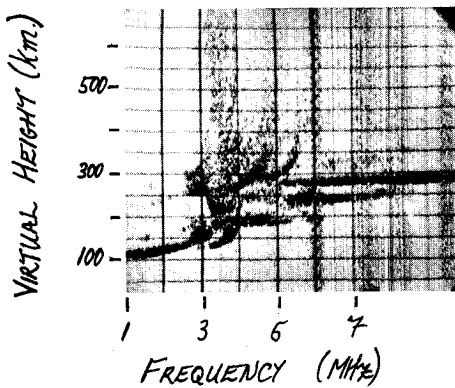
| foF2 | h'F | fxI | type F |
|------|-----|-----|--------|
| F | F | 063 | PF |



1355LT

| foE | foEs | fbEs | h'Es | Es type |
|-----|-------|------|------|---------|
| A | 080JA | 026 | 150 | alrl |

| foF2 | h'F | fxI | type F |
|-------|-----|-----|--------|
| 034UF | 280 | 050 | PF |



1400LT

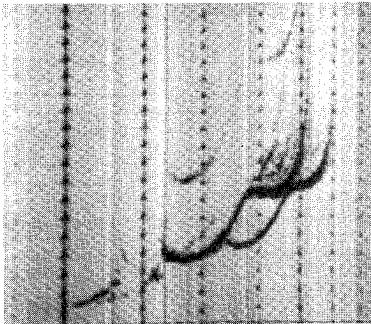
| foE | foEs | fbEs | h'Es | Es type |
|-----|------|------|------|---------|
| A | 032 | 027 | 100 | rl |

| foF2 | h'F | fxI | type F |
|------|-----|-----|--------|
| F | F | 056 | PF |

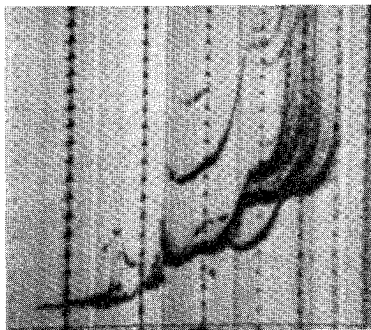
Comment: The oblique Es traces above 200 km have been neglected.

Figure 20 Three ionograms with different receiver gain settings.

The ionograms below from North Pole-8 on 19 August 1961 show the value of having three ionograms with different gain settings in close succession. In this case, the ionogram with minimum gain (1759LT) clearly shows which is the main F region trace, thus foF2 can be measured accurately. It is also interesting to note the effects of gain on other parameters also such as fmin, fm2, and the amount of spread-F present.

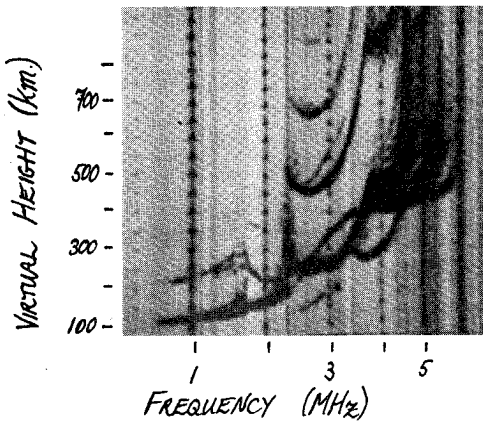


1759LT - LOW GAIN



1800LT - NORMAL GAIN

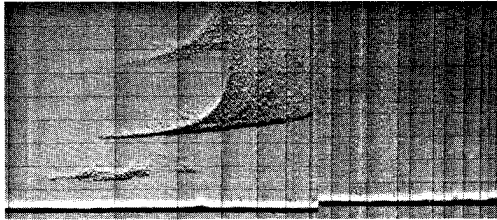
| fmin | foE | foEs | fbEs | h'Es | Es type |
|-------|-------|-------|-------|-------|---------|
| 007-Z | 230-H | O23EG | O23EG | G | - |
| foF2 | h'F2 | h'F | foF1 | fxI | type F |
| O51-F | 400-Q | 230 | 390-L | O60-X | Q1F |



1801LT - HIGH GAIN

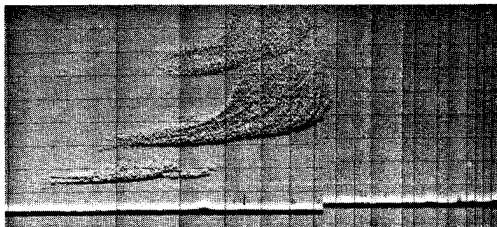
Figure 21 The determination of foF2 from the inner edge of a spread F trace.

The sequence below from Tiksi, recorded on 16 November 1958, illustrates sections 2.71 and 2.72 of the Handbook. Physically a ridge of ionisation has moved over the station and the scaling must take account of this. The scaling foF2 from the inner edge of the spread trace is appropriate at 1905 but not at 1930. Once again the sequence of ionograms and the second order traces provide valuable additional evidence for determining which layer is closer to overhead.



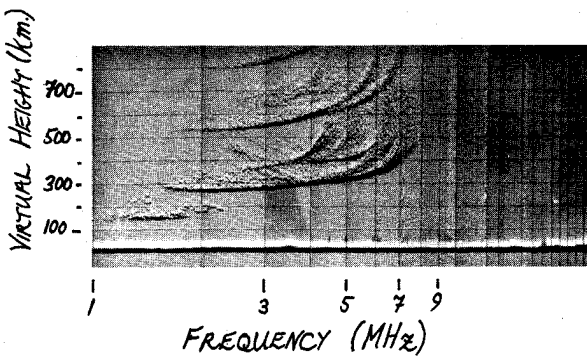
1905LT

| foEs | fbEs | h'Es | Es type |
|-------|------|------|---------|
| 026 | 017 | 115 | rl |
| foF2 | h'F | fxI | type F |
| 042-F | 310 | 080 | F |



1915LT

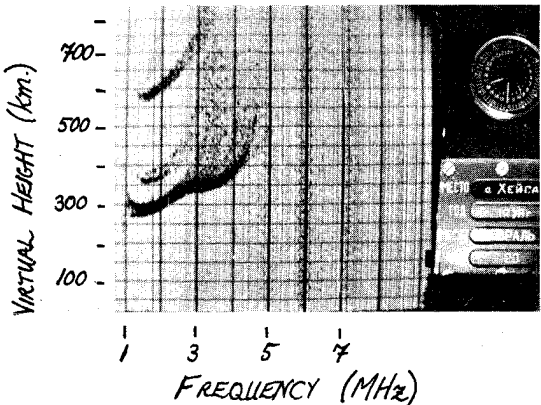
| foEs | fbEs | h'Es | Es type |
|-------|-------|------|---------|
| 027UF | 017 | 115 | rl |
| foF2 | h'F | fxI | type F |
| F | 300-Q | 080 | FQ |



1930LT

| foEs | fbEs | h'Es | Es type |
|-------|-------|------|---------|
| 023 | 016 | 120 | rl |
| foF2 | h'F | fxI | type F |
| 062-F | 265-Q | 080 | Q1F |

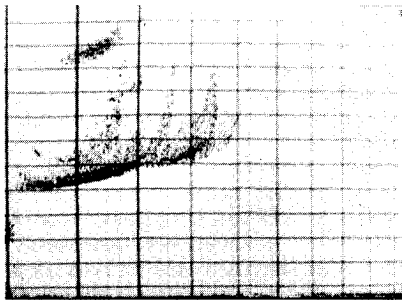
Figure 22 and 23 Further examples of foF2 determination under spread-F conditions.



Heiss 1958 20 February 1630LT (45°E)

| foF2 | h'F | fxI | type F |
|-------|-----|-----|--------|
| 032UF | 275 | 050 | F |

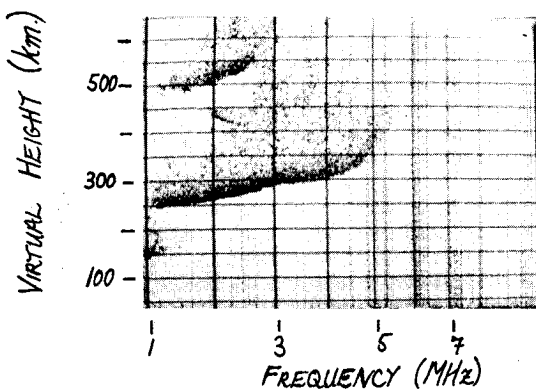
Figure 23 Dixon 28 November 1970



1759LT - LOW GAIN

| foF2 | h'F | fxI | type F |
|------|-----|-----|--------|
| 036 | 250 | - | - |

Comment: No entries have been made for fxI or type F. As these are gain sensitive parameters they must be scaled from the normal gain ionogram.



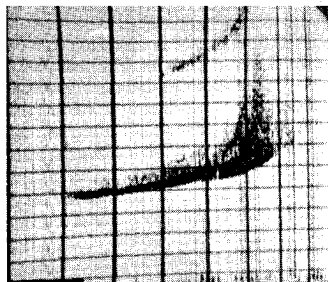
1800LT - NORMAL GAIN

| foF2 | h'F | fxI | type F |
|-------|-----|-----|--------|
| 034DF | 250 | 050 | F |

Comment: Conditions are changing very rapidly with time. The strong trace up to 3.2 MHz is overhead at both 1759 and 1800. It is possible to estimate foF2 by extrapolating from the break between the o- and x-mode traces using the shape of the layer at 1759. This gives foF2 at 3.6 MHz but is uncertain due to the large extrapolation. From the x-trace at 1800 a top limit for foF2 would be 044JF. The true value for foF2 probably lies between these limits but probably closer to 3.6 MHz. Thus foF2 could be scaled as 036DF.

Figure 24 Sequence illustrating large tilts.

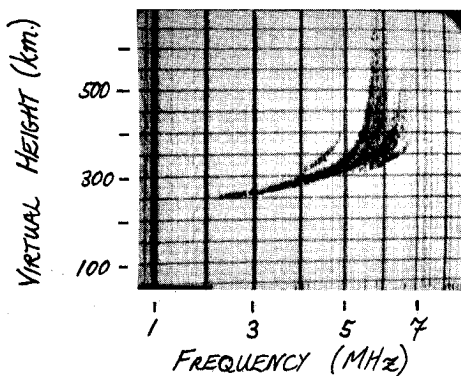
This sequence of ionograms from Dixon recorded on 2 February 1978 shows a trough of ionisation moving over the observatory.



1630LT

| foEs | fbEs | h'Es | Es type |
|-------|-------|------|---------|
| 020EB | 020EB | B | - |

| foF2 | h'F | fxI | type F |
|-------|-----|-----|--------|
| 063-F | 240 | 076 | F |



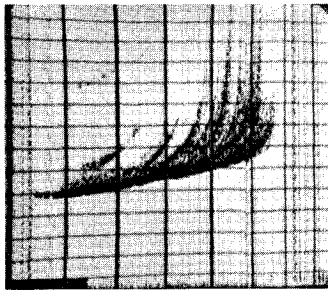
1700LT

| foEs | fbEs | h'Es | Es type |
|-------|-------|------|---------|
| 022EB | 022EB | B | - |

| foF2 | h'F | fxI | type F |
|-------|-----|-----|--------|
| 058-F | 250 | 068 | Q1F |

Comment: z-mode F trace present. fzF2 is 5.0 MHz.

Figure 24 Dixon 28 November 1970



1715LT

| | | | |
|-------|-------|------|---------|
| foEs | fbEs | h'Es | type Es |
| O14EB | O14EB | B | - |
| foF2 | h'F | fxI | type F |
| O54UF | 240 | O68 | Q1F |

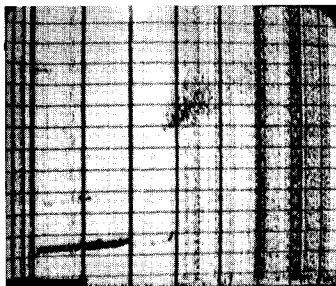
Comment: foF2 in this case is rather difficult to determine uniquely but the quoted value appears most likely.



1745LT

| | | | |
|-------|-------|------|---------|
| foEs | fbEs | h'Es | type Es |
| O23-R | O17 | 150 | rl |
| foF2 | h'F | fxI | type F |
| O28UF | 270EA | O60 | PF |

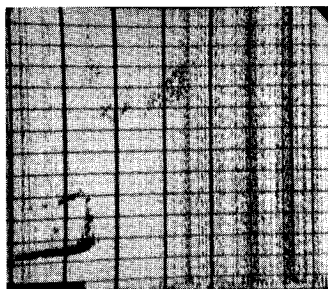
Comment: The original F layer with its critical frequency in excess of 4 MHz is now sufficiently oblique to be regarded as a polar spur trace. Hence the citing of P in the type F column.



1800LT

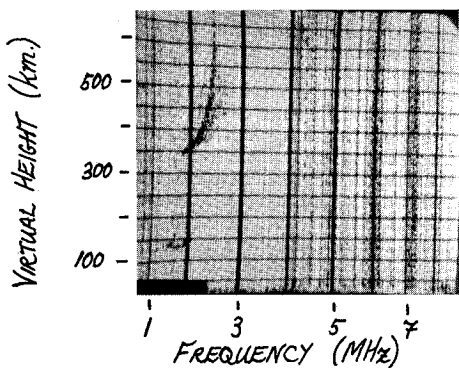
| | | | |
|-------|-------|------|---------|
| foEs | fbEs | h'Es | type Es |
| O30-K | O30AK | 110 | k2 |
| foF2 | h'F | fxI | type F |
| A | A | O50 | P |

Comment: The sequence of ionograms shows that the overhead F layer at 1800 and 1815 LT is completely blanketed by the Es-layer. Thus replacement letters A have been used for foF2 and h'F. fxI is still determined from the polar spur trace which is unaffected by the Es.



1815LT

| | | | |
|-------|-------|------|---------|
| foEs | fbEs | h'Es | type Es |
| O24-K | O24AK | 110 | k2 |
| foF2 | h'F | fxI | type F |
| A | A | O46 | P |



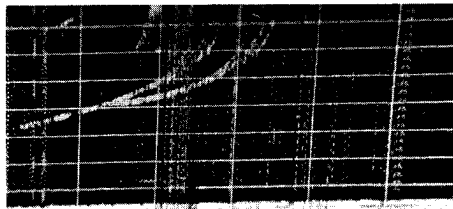
1830LT

| | | | |
|------|-------|-------|---------|
| foEs | fbEs | h'Es | type Es |
| O20 | O18 | 130 | rl |
| foF2 | h'F | fxI | type F |
| O24 | 350EA | O32OB | X |

Comment: The polar spur trace has disappeared leaving only the o-mode F trace from the minimum of the trough.

Figure 25

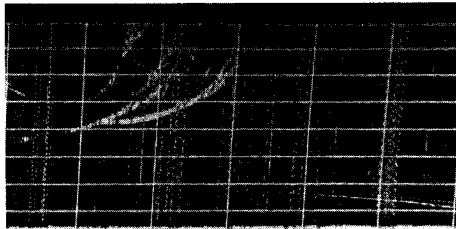
The sequence, from MOSCOW recorded on the 4-5 April 1978, illustrates the passage of the mid latitude electron density trough over a mid-latitude station during a geomagnetically active period. This sequence was originally called a replacement layer sequence and is further illustrated in UAG-50. Once again the main difficulty is in the identification of the overhead F layer.



2115LT

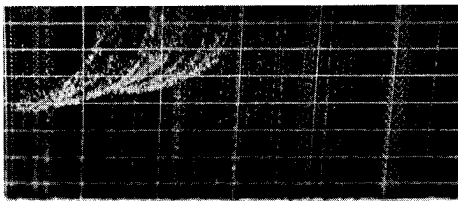
| foF2 | h'F | fxI | type F |
|-------|-----|-------|--------|
| 034-V | 315 | 044-X | Q1X |

Comment: The additional critical frequency at 3.0 MHz shows that there is a very significant tilt present at the high-frequency end of the F layer trace. Hence the entry of Q1 in the type F column. The low-frequency end of the F-layer is nearly horizontal.



2145LT

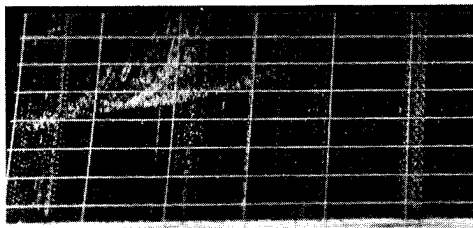
| foF2 | h'F | fxI | type F |
|-------|-----|-------|--------|
| 032-V | 360 | 041-X | Q1X |



2215LT

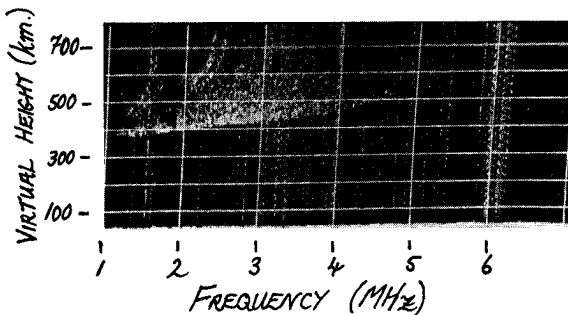
| foF2 | h'F | fxI | type F |
|-------|-----|-----|--------|
| 023-F | 370 | 038 | PF |

Comment: The very weak second order F trace above 700 km suggests that the F layer with the lowest critical frequency is closest to being overhead. This is confirmed by the typical oblique pattern near 2.3 MHz.



2245LT

| foF2 | h'F | fxI | type F |
|-------|-----|-----|--------|
| 022UF | 380 | 043 | PF |

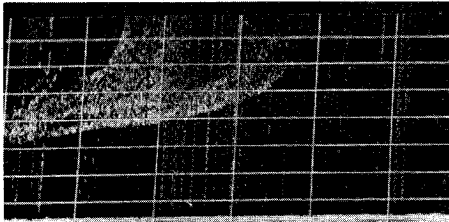


0000LT

| foF2 | h'F | fxI | type F |
|------|-------|-----|--------|
| 016 | 440EE | 047 | PX |

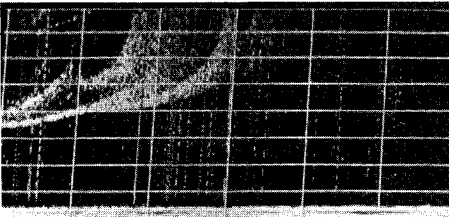
Comment: The combination PX in the type F column is used to indicate that fxI is scaled from a polar spur trace (P) but there is no significant frequency spread present on the overhead F layer (X).

Figure 25 continued Moscow 4-5 April 1978



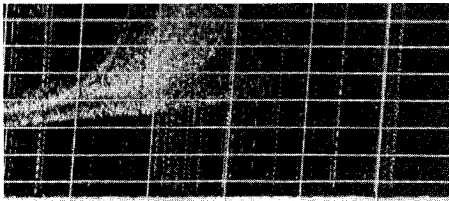
0115LT

| foF2 | h'F | fxI | type F |
|------|-------|-----|--------|
| 017 | 320-Q | 047 | PXQ |



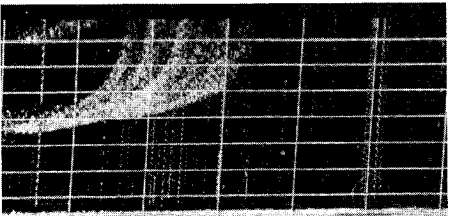
0130LT

| foF2 | h'F | fxI | type F |
|------|-----|-----|--------|
| 019 | 390 | 042 | PX |



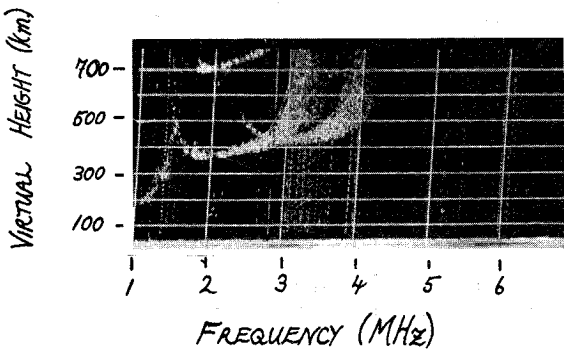
0200LT

| foF2 | h'F | fxI | type F |
|-------|-----|-----|--------|
| 026UF | 340 | 040 | PF |



0345LT

| foF2 | h'F | fxI | type F |
|-------|-------|-----|--------|
| 027UF | 340-Q | 043 | FQ |

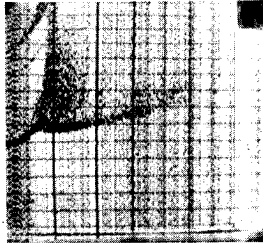


0430LT

| foF2 | h'F | fxI | type F |
|-------|-----|-----|--------|
| 031-F | 350 | 041 | F |

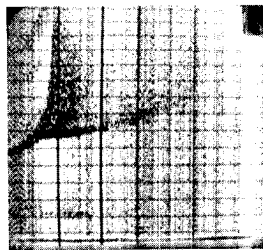
Figure 26 Dixon 4 January 1969

This sequence is taken from a geomagnetically quiet period. There is a polar spur trace present throughout the sequence in the frequency range 2-6 MHz but it remains at oblique incidence.



0530LT

| foF2 | h'F | fxI | type F |
|-------|-------|-----|--------|
| 019-F | 280-E | 060 | PF |



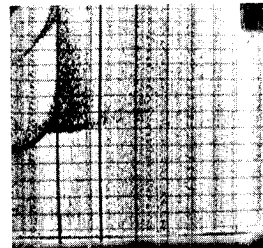
0545LT

| foF2 | h'F | fxI | type F |
|-------|-------|-----|--------|
| 019-F | 280-E | 060 | PF |



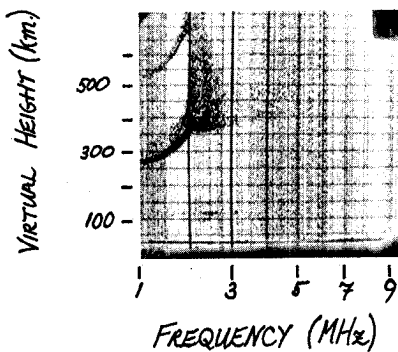
0600LT

| foF2 | h'F | fxI | type F |
|-------|-------|-----|--------|
| 020-F | 275-E | 056 | PF |



0630LT

| foF2 | h'F | fxI | type F |
|-------|-------|-----|--------|
| 020-F | 270-E | 040 | PF |



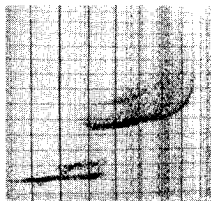
0645LT

| foF2 | h'F | fxI | type F |
|-------|-------|-----|--------|
| 020-F | 260-E | 040 | PF |

Comment: The polar spur trace is rather weak above 2.9 MHz but can be more clearly seen on the original ionogram up to 4.0 MHz

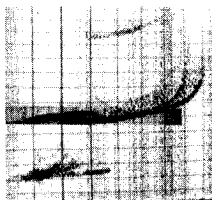
Figure 27 Dixon 24 January 1969

This sequence is taken from a period of moderate geomagnetic activity. The ionograms here should be contrasted with those in Figure 26, which was for quiet conditions. The main differences are that the ridge of ionisation observed obliquely in Figure 26 is now overhead. Also there is significantly more Es of the types associated with particle precipitation.



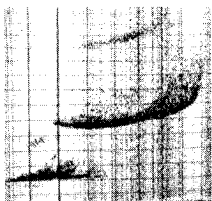
0530LT

| foEs | fbEs | h'Es | Es type |
|-------|-------|-------|---------|
| 036JA | 036-K | 100 | flrl |
| foF2 | h'F | fxI | type F |
| 078JS | 265 | 086-X | FQ |



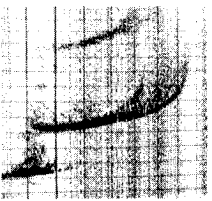
0545LT

| foEs | fbEs | h'Es | Es type |
|-------|-------|-------|---------|
| 034UC | 034UC | 100 | rl |
| foF2 | h'F | fxI | type F |
| 082 | 275 | 090-X | XQ |



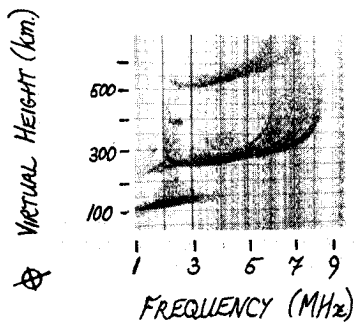
0605LT

| foEs | fbEs | h'Es | Es type |
|-------|-------|------|---------|
| 036UK | 024-K | 100 | rlkl |
| foF2 | h'F | fxI | type F |
| 074UF | 270 | 090 | F |



0630LT

| foEs | fbEs | h'Es | Es type |
|-------|-------|------|---------|
| 021UK | 021-K | 100 | kl |
| foF2 | h'F | fxI | type F |
| 065UF | 250 | 084 | F |

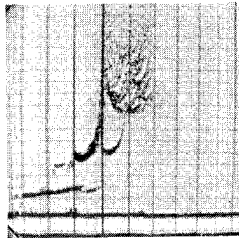


0645LT

| foEs | fbEs | h'Es | Es type |
|-------|-------|-------|---------|
| 025JA | 020-K | 105UA | rlkl |
| foF2 | h'F | fxI | type F |
| 062-F | 250 | 083 | F |

Figure 28 Polar Cusp Precipitation

This sequence from Vostok, Antarctica recorded on 24 January 1970 (summer day) illustrates the effects which are normally observed on ionograms when the polar cusp (or cleft) precipitation is near the station. There is a very significant flux of precipitating particles in the cusp with low energies compared with those observed elsewhere in the auroral oval. These particles mainly stop at F-region heights usually near hmF1 at times within a few hours of magnetic noon.

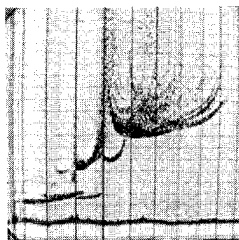


1745LT

| fmin | foE | foEs | fbEs | h'Es | type Es |
|------|-------|-------|-------|------|---------|
| 010 | 300UY | 030EG | 030EG | G | - |

| foF2 | h'F2 | h'F | foF1 | fxI | type F |
|------|------|-----|------|-----|--------|
| F | Q | 255 | 400 | 060 | FQ |

Comment: The overlapping normal E and F traces near foE indicate there is a severe tilt present (see UAG 23A p 50). It is not possible to decide from these small reproductions whether it is this E or the F layer which is tilted, but UY has been used on foE on this occasion.

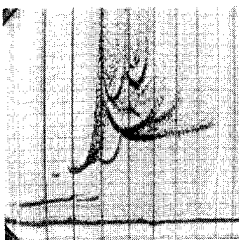


1750LT

| fmin | foE | foEs | fbEs | h'Es | type Es |
|------|-------|-------|-------|------|---------|
| 010 | 300-Y | 030EG | 030EG | G | - |

| foF2 | h'F2 | h'F | foF1 | fxI | type F |
|------|-------|-----|-------|-----|--------|
| F | 390DQ | 250 | 400-F | 095 | PFQ |

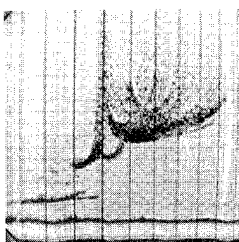
Comment: Note the presence of a z-mode F-trace near 2.5 MHz.



1800LT

| fmin | foE | foEs | fbEs | h'Es | type Es |
|------|-------|-------|-------|------|---------|
| 010 | 290UY | 029EG | 029EG | G | - |

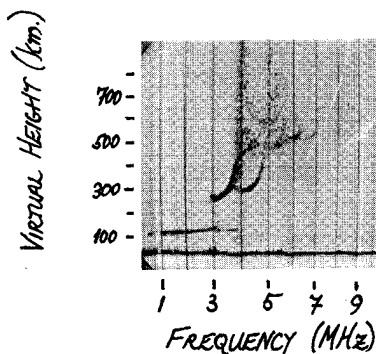
| foF2 | h'F2 | h'F | foF1 | fxI | type F |
|-------|------|-----|-------|-----|--------|
| 049UF | 550 | 250 | 400-F | 080 | PFQ |



1815LT

| fmin | foE | foEs | fbEs | h'Es | type Es |
|------|-------|-------|-------|------|---------|
| 010 | 280ZY | 028EG | 028EG | G | - |

| foF2 | h'F2 | h'F | foF1 | fxI | type F |
|------|-------|-----|-------|-----|--------|
| F | 370-Q | 255 | 390-F | 094 | PFQ |



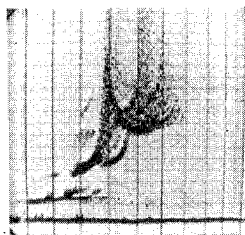
1830LT

| fmin | foE | foEs | fbEs | h'Es | type Es |
|------|-------|-------|-------|------|---------|
| 010 | 290EY | 028EG | 028EG | G | - |

| foF2 | h'F2 | h'F | foF1 | fxI | type F |
|------|------|-----|-------|-----|--------|
| F | Q | 250 | 390-F | 070 | FQ |

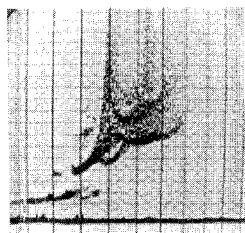
Figure 29 Station moving under the polar cusp during the summer.

When a station moves under the cusp in summer, the entire F-layer traces are very severely affected. The most readily identifiable feature is a rapid rise in the maximum plasma frequency of the F2 layer, with an associated fall of hmF2 to near hmF1. The cusp F-layer traces show considerable range and frequency spread-F. The sequence of ionograms below recorded at Vostok on 22 January 1970 show all these features as the station moves under the polar cusp. The ionogram at 1945LT is typical for overhead cusp precipitation.



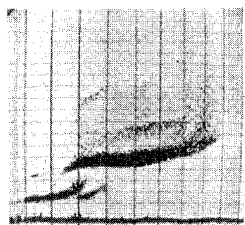
1905LT

| fmin | foE | foEs | fbEs | h'Es | Es type |
|-------|-------|-------|-------|------|---------|
| 010 | 26OUF | 026EG | 026EG | G | - |
| foF2 | h'F2 | h'F | foF1 | fxI | type F |
| 051DF | Q | 220 | 390-F | 070 | PFQ |



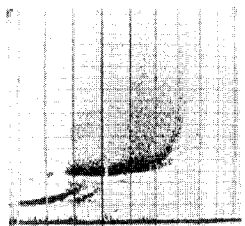
1915LT

| fmin | foE | foEs | fbEs | h'Es | Es type |
|-------|-------|-------|-------|------|---------|
| 010 | 26OUY | 026EG | 026EG | G | - |
| foF2 | h'F2 | h'F | foF1 | fxI | type F |
| 053DF | Q | 225 | 400-F | 070 | PFQ |



1945LT

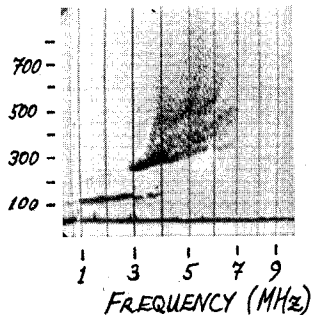
| fmin | foE | foEs | fbEs | h'Es | Es type |
|------|------|-------|-------|------|---------|
| 010 | Y | 026EG | 026EG | G | - |
| foF2 | h'F2 | h'F | foF1 | fxI | type F |
| Q | Q | 240EY | Q | 090 | Q |



2000LT

| fmin | foE | foEs | fbEs | h'Es | Es type |
|------|------|-------|-------|------|---------|
| 010 | Y | 025EG | 025EG | G | - |
| foF2 | h'F2 | h'F | foF1 | fxI | type F |
| Q | Q | 230-Q | Q | 072 | Q |

VIRTUAL HEIGHT (km.)

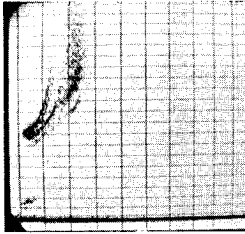


2015LT

| fmin | foE | foEs | fbEs | h'Es | Es type |
|-------|------|-------|-------|-------|---------|
| 010 | Y | 025EG | 025EG | G | - |
| foF2 | h'F2 | h'F | foF1 | fxI | type F |
| 054UF | Q | 250 | 400UF | 0640B | PFQ |

Figure 30 Station moving under the polar cusp in winter.

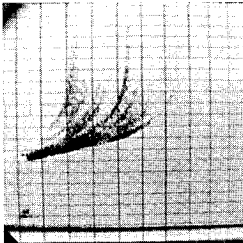
This sequence of ionograms, from Vostok on 27 June 1970, shows the station moving under the polar cusp under winter conditions. For this station in winter, there is no solar illumination of the E or F-layers at times when the polar cusp may be present. However, the similarity between the F-region traces at 2005LT in this example and 1945LT on Figure 29 recorded in summer is remarkable.



1905LT

| foF2 | h'F | fxI | type F |
|-------|-----|-------|--------|
| 023UF | E | 043OB | F |

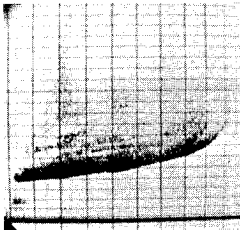
Comment: normal winter ionogram.



1930LT

| foF2 | h'F | fxI | type F |
|-------|-------|-----|--------|
| 032UF | 350-Q | 082 | PFQ |

Comment: Cusp precipitation at oblique incidence.



2005LT

| foF2 | h'F | fxI | type F |
|------|-------|-----|--------|
| Q | 230-Q | 102 | Q |

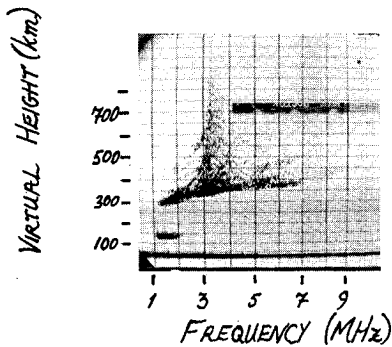
Comment: Cusp precipitation overhead.



2030LT

| foF2 | h'F | fxI | type F |
|-------|-----|-----|--------|
| 032UF | Q | 090 | PFQ |

Comment: The identification of foF2 at 3.2 MHz would be very doubtful using this ionogram alone. Additional information from unpublished ionograms must have been used to allow the determination of the value of foF2.



2055LT

| foF2 | h'F | fxI | type F |
|-------|-----|-----|--------|
| 032UF | 280 | 090 | PF |

